IEEE Photonics Journal
An IEEE Photonics Society Publication

Open Access

Reconfigurable Unidirectional Photonic Crystal Using Liquid Crystal Layer

Volume 9, Number 1, Febuary 2017

Aya El-metwally
Nihal F. F. Areed
Mohamed Farhat O. Hameed, ***Senior Member, IEEE***
Salah S. A. Obayya, ***Senior Member, IEEE***

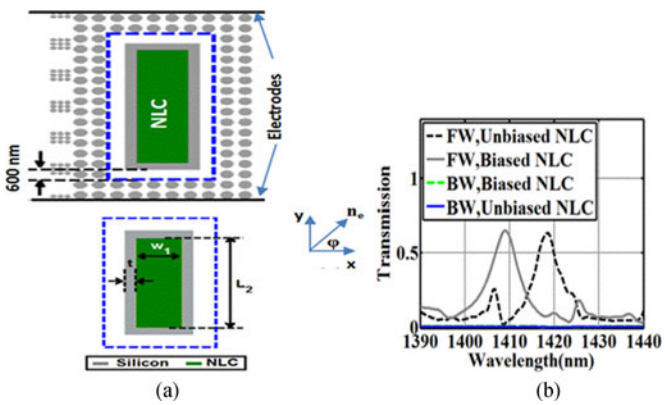

DOI: 10.1109/JPHOT.2016.2638045
1943-0655 © 2016 IEEE

IEEE photonics SOCIETY

IEEE

Reconfigurable Unidirectional Photonic Crystal Using Liquid Crystal Layer

Aya El-metwally,[1,2] **Nihal F. F. Areed,**[1,2]
Mohamed Farhat O. Hameed,[1,3] ***Senior Member, IEEE*,**
and Salah S. A. Obayya,[1,2] ***Senior Member, IEEE***

[1]Center for Photonics and Smart Materials, Zewail City of Science and Technology, Sheikh Zayed District,12588, 6th of October City, Giza, Egypt (Email: sobayya@zewailcity.edu.eg)
[2]Electronics and Communications Engineering Department, Faculty of Engineering, Mansoura University, Mansoura, 35516, Egypt
[3]Mathematics and Engineering Physics Department, Faculty of Engineering, Mansoura University, Mansoura, 35516, Egypt

DOI:10.1109/JPHOT.2016.2638045

Manuscript received October 27, 2016; revised December 5, 2016; accepted December 7, 2016. Date of publication December 9, 2016; date of current version December 28, 2016. Corresponding author: S. S. A. Obayya (e-mail: sobayya@zewailcity.edu.eg).

Abstract: Reconfigurable unidirectional transmission based on the nematic liquid crystal (NLC) layer and 2-D photonic crystal (PhC) platforms is presented and simulated. The suggested one way transmission can be tuned at different wavelengths based on the NLC biasing state. A comprehensive parametric study using plane wave expansion and finite difference time domain (FDTD) methods has been carried out for explaining and optimizing the performance of the proposed structure. The transmission spectra calculations reveal that the reported structure can perform nearly perfect isolation at two different bands (1406–1412 nm and 1416–1421 nm) with an average contrast ratio (Cr) of about 36.9 dB. The investigated unidirectional PhC structure has advantages in terms of compactness and reconfigurability and can be used efficiently in ultrahigh nanoscale integrated circuits.

Index Terms: Integrated optic, photonic crystals, liquid crystal.

1. Introduction

Unidirectional transmission device is needed to isolate the source from back reflections in many potential applications such as biomedical imaging [1], optical communication [2], quantum computers [3], and photonic integrated circuits (PICs). As reported in [1], the One way transmission device is needed to prevent the light back-reflection in optical coherence tomography (OCT) that performs real time in vivo cross-sectional tomograms of skin, esophagus and coronary artery. Further, as reported in [4], one way transmission device is mandatory for implementation of image encryption system.

The traditional mechanism to realize optical isolation is via magneto-optic materials, in which large number of elements should be deposited on polycrystalline films [5]–[7]. However, such technique suffers from integration difficulty with recent integrated photonic systems [8]. Recently, number of alternative and more compact approaches based on different physical principles such as, non-linear optics [9]–[11], metamaterials [12]–[14], plasmonics [15], [16], and photonic crystals (PhCs) with pseudo-bandgaps [17]–[19] have been reported. Based on these studies, it can be concluded that plasmonic isolators have practically narrow operating frequency band while the implemented isolators using PhC platforms have lower isolated contrast ratio of around 15 dB with higher

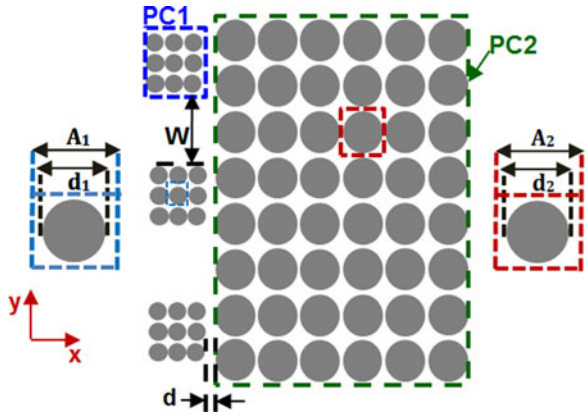

Fig. 1. Schematic diagram of the proposed unidirectional transmission structure. The geometrical parameters of the PhC#1 and PhC#2 unit cells are defined in the cyan and red rectangles, respectively.

losses. Recently, an alternative unidirectional device based on silicon grating and PhC with pseudo-bandgap has been reported [20]. Such structure is simple, compact and offers efficient isolation over a wide range of frequency with high contrast ratio of around 18.7 dB at frequency of 220.5 THZ. Nowadays, one of the greatest challenges is to have reconfigurable photonic devices. Injection of liquid crystal (LC) materials in the PhC platform cavities is commonly employed for controlling the operation of the optical devices [21]–[23]. The orientation of the LC molecules and hence the refractive index of LC can be modulated with the effect of temperature and/or an external electric field [24]–[26].

In this paper, we propose and simulate reconfigurable one-way optical transmission based on nematic LC (NLC) layer and 2-D PhC platform. Firstly, to allow one way transmission, integration between two PhC structures is suggested. The first PhC structure PhC#1 that is composed of nine circular rods arranged in a square lattice is repeated along one dimension with spacing of 1130 nm. Such PhC pattern is inserted on the left of another square lattice PhC structure with different dimensions (PhC#2). To allow isolation reconfigurability at different operating wavelength zones, hollow rectangular Si pan infiltrated with NLC layer is inserted in the midway of the considered PhC platform (PhC#2). Detailed descriptions of the proposed structure are given in the next sections. All simulation results such as band structure and transmission spectra have been calculated using plane wave expansion (PWE) [27] and 2-D finite difference time domain (FDTD) [28] methods, respectively. The transmittance through the one-way device based on the combination between PhC#1 and PhC#2 only shows that a light with wavelength ranging from 1355–1375 nm can be passed from the front side. However, such wavelength range will be totally reflected by the structure from the back-side with contrast ratio of around 39.2 dB. On the other hand, the integration between the PhC#1, PhC#2 and NLC layer enables one way transmission at two different bands centered at 1409 nm and 1419 nm according to the NLC biasing state. The proposed unidirectional transmission structure is attractive as it can be effectively employed for the optical isolation in image encryption systems [29] and medical instruments, such as the blood gas analyzer [30].

2. Unidirectional Phc and Design Concept

Fig. 1 shows the schematic configuration of the first proposed optical isolator. It consists of two types of two-dimensional PhC finite components PhC#1 and PhC#2. The silicon rods of the PhC#1 of diameter $d1 = 210$ nm are arranged in a square lattice with lattice constant of $A1 = 230$ nm. However, the PhC#2 consists of silicon rods of diameter $d2 = 450$ nm with a lattice constant $A2 = 600$ nm. The component PhC#1 is repeated along y-axis with spacing $w = 1.13\,\mu$m and the repeated pattern is inserted on the left of component PhC#2. The distance between PhC#1

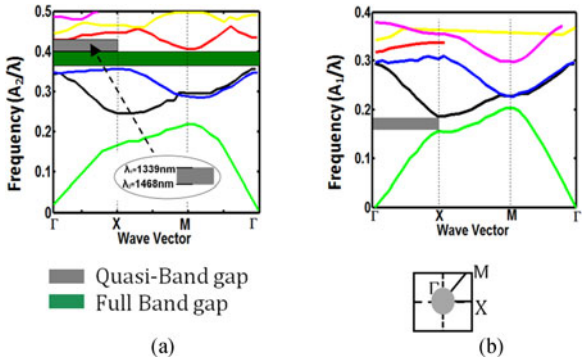

Fig. 2. Band structures of the platforms (a) PhC#2 and (b) PhC#1.

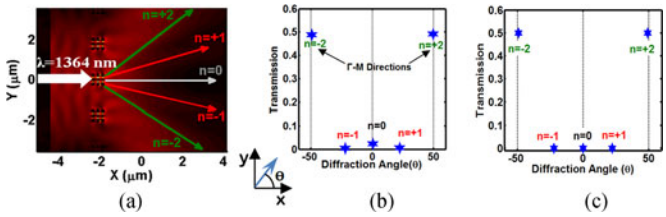

Fig. 3. Light diffraction through the proposed structure at $\lambda = 1364$ nm. The transmitted diffraction pattern after PC#1 (a) steady state field distribution, (b) fraction of the transmitted power to each physical grating order, and (c) transmitted diffraction pattern after PC#2 structure.

and PhC#2 is d = 93 nm, and the refractive index of silicon is set to 3.49. Silicon is an abundant element and is commonly used in several applications such as implementing of photonic crystal devices [31]–[35] and solar energy harvesters [36].

First, to explain the physical operation of the proposed unidirectional transmission device, PWE method [27] is employed to calculate the band structures of the PhC platforms PhC#1 and PhC#2. It is found that there exists a quasi-bandgap (gray region) ranging from $A_2/\lambda = 0.448$ to 0.4086 ($\lambda = 1339$ nm to 1468 nm) for PhC#2 as shown in Fig. 2(a). Such quasi-bandgap means that the light can be propagated along M-Γ direction with no light propagation along Γ-X direction. It is worth noting that an array of PhC#1components has been adopted instead of conventional grating reported in [20] to change the direction of the incident light ranging from ($\lambda = 1355$ nm to 1375 nm) along Γ-X direction (stop band) to M-Γ direction (pass band) and to pass the light through the composite structure. The importance of the proposed modification can be identified with the aid of the calculated band structure shown in Fig. 2(b), which shows that PhC#1 has quasi-bandgap (gray region) ranging from $A_1/\lambda = 0.1556$ to 0.1862 ($\lambda = 1234$ nm to 1478 nm). Therefore, the use of the PhC#1 components will minimize the transmittance through the Γ-X direction in the forward propagation and consequently narrow optical isolation band can be obtained as will be shown later in Fig. 4 discussion.

Fig. 3 studies the effect of the array of PhC#1 components on the light propagation through the proposed design. As evident from Fig. 3(a), the PhC#1 can split the incident light with wavelength $\lambda = 1364$ nm from gray region in Fig. 2(a) into several beams travelling in different directions. The electric field passes through the periodic PhC#1 platform and is divided into 3 diffracted orders (n = 0, n = $\pm$1, n = $\pm$2). Further, the fraction of the transmitted power to each physical diffracted order is calculated for a given platform as shown in Fig. 3(b).The transmission is normalized such that the sum of all orders is equal to 1. It may be seen from Fig. 3(b) that the transmission for zeroth order (Γ-X direction) and 1st order are approximately equal to zero. On the other hand, each of the 2nd grating orders (Γ-M direction) has large transmission of about 0.49. As a result, the light entering form the PhC#1 side (forward direction) is allowed. However, the incident light form PhC#2

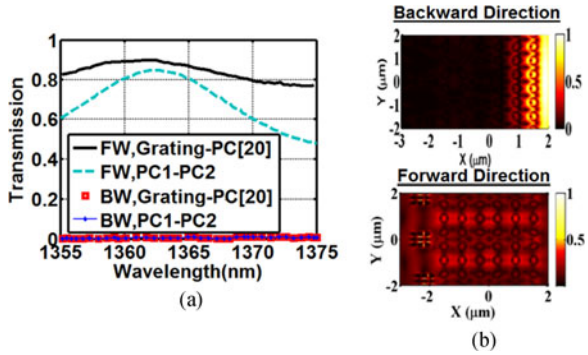

Fig. 4. (a) Transmission spectra in the forward and backward directions of the proposed unidirectional transmission device and that reported in [20]. (b) Field distributions through the suggested design in backward and forward direction.

interface (backward direction) is blocked. Additionally, Fig. 3(c) shows the transmitted diffraction pattern after the component PhC#2 at $\lambda = 1364$ nm. It is clearly evident from the figure that the transmission for the zeroth order (Γ-X direction) and first order are equal to zero while, each of the second grating orders (Γ-M direction) has a large transmission of about 0.5. It is worth noting that there is a good agreement between the calculated diffraction pattern and the band structure diagram shown in Fig. 2(a), where the PhC#2 structure allows only the propagation along Γ-M direction.

Next, 2-D FDTD method based on Lumerical software [28] has been applied for calculating the forward and backward transmission spectra through the proposed structure. A computational window of size 1 μm $\times$ 1 μm $\times$ 7.91 μm has been discretized with a uniform mesh where the grid spacing are chosen as ($\Delta x = \Delta y = 10$ nm). Further, the computational window is bounded from all sides by 500 nm thickness of perfectly matched layer (PML) absorbing boundary conditions. Figure 4(a) shows the calculated transmission spectra of a TM polarized light normally incident from PhC#1 side (forward, cyan line) and PhC#2 side (backward, blue line). Additionally the figure shows the calculated forward and backward transmission spectra of the previously reported grating-PhC structure [20]. It is evident from this figure that in the forward propagation, the transmission spectrum of the proposed (PhC#1-PhC#2) structure is mush narrow than the spectrum of the previously reported (grating-PhC)structure [20]. This can be rooted to the use of the 1D array of the PhC#1 components. It is also abbreviated from Fig. 4 that the transmission of light through the proposed unidirectional transmission device in the forward direction forms relatively sharp peak of about 0.836 at wavelength of 1364 nm, while the transmission in the backward direction is around 0.0001. The contrast ratio (C_r) has been employed to quantify the performance of the reported structure, and it is given by

$$\text{Contrast ratio } (C_r) = 10 \log \left(\frac{F}{B} \right) \tag{1}$$

where F and B are the forward and the backward transmissions, respectively.

Based on the transmission calculations, the proposed structure enables one way transmission with C_r of about 39.2 dB at $\lambda = 1364$ nm. The isolation capabilities of the reported unidirectional transmission structure are more evident by the captured field distributions at $\lambda = 1364$ nm in the forward and backward directions shown in Fig. 4(b). The displayed fields clearly agree with the simulated transmission results where the incident light from PhC#1 side can propagate through the structure while the incident light form PhC#2 side is completely reflected back by the PhC#2.

Next, to allow isolation reconfigurability between two different operating wavelength regimes, the combination between the NLC and the studied unidirectional transmission in PhC structure is presented as shown in Fig. 5. By studying the geometrical parameters and biasing states of the

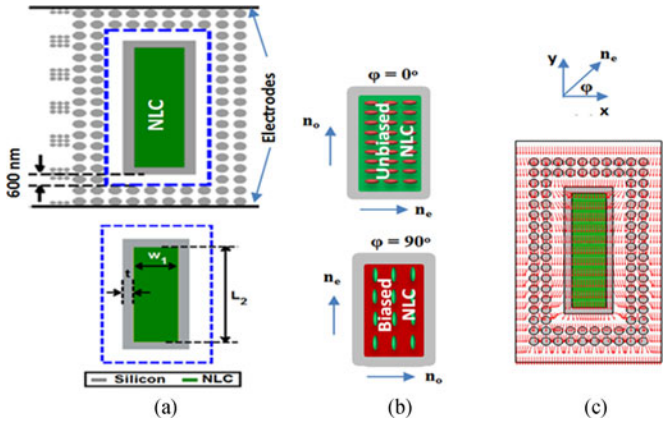

Fig. 5. (a) Proposed reconfigurable unidirectional PhC structure. (b) NLC molecular orientation for biased and unbiased states. (c) E-field distribution across the proposed structure.

NLC layer, it will be easy to control the position of the transmission peak of the dashed line shown in Fig. 4(a) and thereby one way transmission behavior at different wavelength bands can be obtained.

3. Reconfigurable Unidirectional Phc Structure

Fig. 5 shows the suggested reconfigurable unidirectional transmission structure based on 2D-PhC platform with the NLC layer. As shown in Fig. 5, hollow rectangular Si pan (gray rectangular) infiltrated with NLC layer of type E7 is inserted in the midway of PhC#2 structure. The distance between the Si pan with wall thickness t = 375 nm and dashed blue rectangular is equal to 600 nm. The orientation of the NLC molecules and the NLC refractive index can be modulated by applying an external electric field. Figure 5(a) shows a proposal for electrodes alignment in which the two electrodes are aligned along y axis to modulate the biasing state of the NLC layer. The relative permittivity tensor ε_r of the E7 is taken as [37]

$$\varepsilon_r = \begin{pmatrix} n_o^2\sin^2\varphi + n_e^2\cos^2\varphi & (n_e^2 - n_o^2)\cos\varphi\sin\varphi & 0 \\ (n_e^2 - n_o^2)\cos\varphi\sin\varphi & n_o^2\cos^2\varphi + n_e^2\sin^2\varphi & 0 \\ 0 & 0 & n_o^2 \end{pmatrix} \quad (2)$$

where φ is the rotation angle of the NLC director, which can be controlled by using electric electrodes, as shown in Fig. 5(b).

In the NLC unbiased state, the director of NLC molecules is aligned along x-axis with rotation angle $\varphi = 0^\circ$. Therefore, the light polarized in y-direction depends on the ordinary index n_o. However, in the heavily biased state, the NLC molecules are aligned with a rotation angle $\varphi = 90^\circ$. In this case, the y-polarized light is affected by the extraordinary index n_e. The injection of the NLC can be applied by the very precise technique reported in [38]. This technique is based on utilizing a micropipette with outer diameter tip that is computer controlled by a 3 axis Eppendorf TransferMan NK 2micro-manipulator.

Additionally, in order to ensure that the alignment of the NLC molecules can be obtained successfully, an important analysis is made where Gauss law is solved along with the electric potential electric field relation given by $\nabla \cdot D = \rho$ and $E = -\nabla V$, where D is the displacement field, E is the electric field, V is the electric potential, and ρ is the charge density which is equal to zero for a dielectric material. The FVFEM based on Comsol Multiphysics Software [39] is used to solve the two equations over a rectangular shaped computational domain (7.2 μm $\times$ 12.6 μm). The electrodes voltage is taken as 100 V which is greater than the Fréedericksz threshold [40]. In this study, the degree of freedom is equal to 68559 with minimum element size of 3.78 nm and Dirichlet boundary

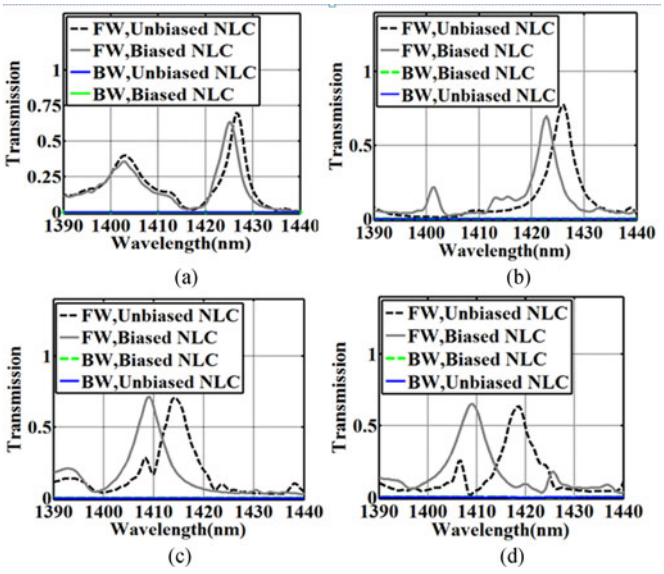

Fig. 6. Transmission spectra at different cross section areas of NLC.

conditions for the electric potential. It may be seen from Fig. 5(c) that the electric potential and the electric field are uniform inside the NLC region. Therefore, the surrounding PhC structures will not affect the uniformity of the electric field through the NLC.

Comprehensive parametric study has been carried out to achieve one way transmission that can be configured to function at different wavelength zones based on the biasing state of the NLC layer. Figure 6 shows the calculated forward and backward transmission with respect to the wavelength with different NLC cross section areas. It can be noted from these figures that the shift between the peaks of the transmission for biased and unbiased NLC can be increased from 2 nm up to 10 nm by increasing the cross sectional area of the NLC layer from 1.87 to 11.05 μm^2. The figure of merit (FOM) based on the spectral shift ($\lambda_2 - \lambda_1$) and the half power beam width (HPBW) of the transmitted beam at the biased NLC has been employed to quantify the performance of proposed reconfigurable unidirectional structure as follows:

$$\text{FOM} = \frac{\boldsymbol{\lambda_2 - \lambda_1}}{\textbf{HPBW}} \tag{3}$$

where λ_1 and λ_2 are the centers of the transmitted bands at the heavily biased and unbiased states, respectively.

The calculated transmission with small NLC area offers forward transmission at $\lambda_1 = 1425$ nm with HPBW $= 5$ nm at heavily biased state and forward transmission at $\lambda_2 = 1427$ nm at the unbiased state as shown in Fig. 6(a). Consequently, the FOM value reads 0.4. However, using cross sectional area of 7.15 μm^2 results in FOM of about 0.8 where the spectral shift and the HPBW are equal to 5 nm and 6 nm, respectively as shown in Fig. 6(b). Moreover, by increasing the width w_1 to 1.7μm, the FOM reads 0.75 as shown in Fig. 6(c). In order to further increase the FOM, we have increased the area of the NLC layer to 11.05 μm^2 as shown in Fig. 6(d). It may be noted from Fig. 6(d) that the values of the spectral shift, HPBW and FOM are equal to10 nm, 7 nm and 1.42, respectively.

Additionally, the impact of the continuous variation between the ordinary and extraordinary refractive indices on the performance of the proposed reconfigurable unidirectional PhC structure has been investigated as shown in Fig. 7. The figure illustrates that increment of the rotation angle φ of NLC director between $\varphi = 0^\circ$ and $\varphi = 90^\circ$ shifts the unidirectional band towards longer wavelengths.

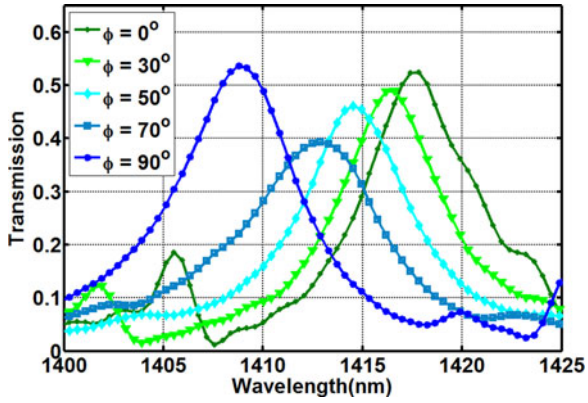

Fig. 7. Transmission spectra through the proposed structure at different rotation angles of NLC director.

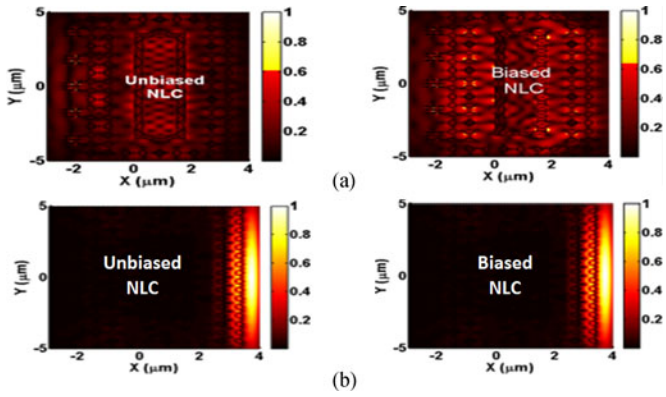

Fig. 8. Steady state field distributions at $\lambda = 1409$ nm and $\lambda = 1419$ for unbiased biased NLC in (a) the forward direction and (b) the backward direction.

Fig. 8(a) and (b) shows the captured electric field distributions at $\lambda = 1409$ nm and $\lambda = 1419$ nm in the forward and the backward directions for heavily biased NLC and unbiased NLC, respectively. It can be observed that the field distributions clearly agree with the transmission spectra behavior, where the incident light from PhC#1 side can propagate through the structure while the incident light form PhC#2 side is completely reflected back by the PhC#2.

The tolerance with respect to the fabrication errors has been also investigated. The variation in all geometrical parameters by the percentage, Δ and its impact on the FOM and C_r has been evaluated and plotted as shown in Fig. 9(a). For example, with increasing all parameters (A_1, d_1, A_2, d_2, L_2, w_1 and d) by $+5\%$, the FOM and C_r read 1.42 and 36.9 dB, respectively. We can see from the figure that the overall acceptance tolerance will be within $\pm 5\%$ where the acceptable FOM values are within the range of 1.28:1.42 with minimum variation in the C_r within the range of 35:38 dB. Further, the performance of the proposed reconfigurable unidirectional PhC structure at different the temperatures has been studied. Fig. 9(b) shows the impact of temperature variation from 15 °C to 50 °C on the contrast ratio C_r. It may be noted from this figure that the temperature variation slightly affects the performance of the proposed structure with no more than 1% variation in the C_r value. Finally, the tolerance with respect to the errors in obtaining the heavily biased NLC ($\varphi = 90^\circ$) the unbiased NLC ($\varphi = 0^\circ$) has been evaluated. Fig. 9(c) shows the variations in the directional angle $\varphi = 90^\circ$ and 0^o of the NLC molecules by $\Delta\varphi$ and their impact on the contrast ratio. As may be observed from the figure, there is a tolerance of $\Delta\varphi = 5^\circ$ at which a slight degradation in the C_r value form 37.4 dB to 37.1dB.

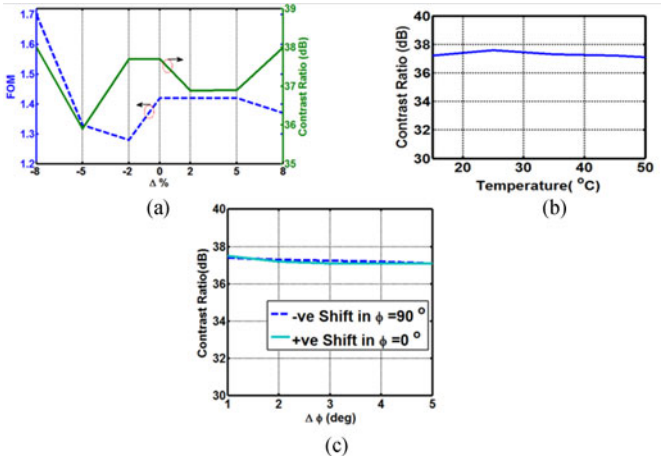

Fig. 9. (a) Contrast ratio and FOM versus fabrication tolerance for unbiased NLC state. (b) Variation of the contrast ratio with the temperature. (c) Variation of the contrast ratio with the rotation angle of the NLC director (φ).

4. Conclusion

We have presented and simulated unidirectional transmission PhC structure with C_r of about 39.2 dB at $\lambda = 1364$ nm. Additionally, the proposed structure has been integrated with NLC layer to obtain reconfigurable one-way optical transmission device. Hollow rectangular Si pan infiltrated with NLC layer of type E7 is inserted in the midway of the PhC#2. Reconfigurable optical isolator can be configured to isolate different operating wavelengths based on the biasing state of the NLC layer. The simulation results reveal that the proposed structure can perform nearly perfect isolation at two different bands centered at 1409 nm and 1419 nm with an average contrast ratio (C_r) of about 36.9 dB. Further, the fabrication tolerances of the suggested devices show that the fabrication errors need to be controlled with no more than $\pm$5%. The proposed unidirectional transmission based NLC can be exploited to implement key functionalities required in different applications such as biomedical imaging and optical communication.

References

[1] S. R. Chinn, E. A. Swanson, and J. G. Fujimoto, "Optical coherence tomography using a frequency-tunable optical source," *Opt. Lett.* vol. 22, no. 5, pp. 340–342, 1997.
[2] J. L. O'Brien, G. J. Pryde, A. G. White, T. C. Ralph, and D. Branning, "Demonstration of an all-optical quantum controlled-NOT gate," *Nature*, vol. 426, pp. 264–267, Nov. 2003.
[3] E. Knill, R. Laflamme, and G. J. Milburn, "A scheme for efficient quantum computation with linear optics," *Nature*, vol. 409, pp. 46–52, 2001.
[4] N. F. F. Areed and S. S. A. Obayya, "Multiple image encryption system based on nematic liquid photonic crystal layers," *J. Lightw. Technol.*, vol. 32, no. 7, pp. 1344–1350, Apr. 2014.
[5] M. Levy, J. R. M. Osgood, H. Hegde, F. J. Cadieu, R. Wolfe, and V. J. Fratello, "Integrated optical isolators with sputter-deposited thin-film magnets," *IEEE Photon. Technol. Lett.*, vol. 8, no. 7, pp. 903–905, Jul. 1996.
[6] H. Shimizu and Y. Nakano, "Monolithic integration of a waveguide optical isolator with a distributed feedback laser diode in the 1.5-μm wavelength range," *IEEE Photon. Technol. Lett.*, vol. 19, no. 24, pp. 1973–1975, Dec. 2007.
[7] L. Bi, J. Hu, P. Jiang, D. Kim, G. Dionne, L. Kimerling, and C. Ross, "On-chip optical isolation in monolithically integrated non-reciprocal optical resonators," *Nature Photon.*, vol. 5, pp. 1–5 2011.
[8] C. R. Doerr, L. Chen, and D. Vermeulen, "Silicon photonics broadband modulation-based isolator," *Opt. Exp.*, vol. 22, pp. 4493–4498, 2014.
[9] M. Soljačić, C. Luo, J. D. Joannopoulos, and S. Fan, "Nonlinear photonic crystal microdevices for optical integration," *Opt. Lett.*, vol. 28, pp. 637–639, 2003.
[10] K. Gallo, G. Assanto, K. R. Parameswaran, and M. M. Fejer, "All-optical diode in a periodically poled lithium niobate waveguide," *Appl. Phys. Lett.*, vol. 79, 2001, Art. no. 314.
[11] L. Fan *et al.*, "An all-silicon passive optical diode," *Science*, vol. 335, pp. 447–450, 2012.

[12] Y. D. Xu, C. D. Gu, B. Hou, Y. Lai, J. Li, and H. Y. Chen, "Broadband asymmetric waveguiding of light without polarization limitations," *Nature Commun.*, vol. 4, 2013, Art. no. 2561.
[13] M. Mutlu, A. E. Akosman, A. E. Serebryannikov, and E. Ozbay, "Diode like asymmetric transmission of linearly polarized waves using magnetoelectric coupling and electromagnetic wave tunneling," *Phys. Rev. Lett.*, vol. 108, no. 21, May 2012, Art. no. 213905.
[14] C. Menzel *et al.*, "Asymmetric transmission of linearly polarized light at optical metamaterials," *Phys. Rev. Lett.*, vol. 104, Jun. 2010, Art. no. 253902.
[15] E. Battal, T. A. Yogurt, and A. K. Okyay, "Ultrahigh contrast one-way optical transmission through a subwavelength slit," *Plasmonics*, vol. 8, 2013, Art. no. 509.
[16] S. Cakmakyapan, A. E. Serebryannikov, H. Caglayan, and E. Ozbay, "One-way transmission through the subwavelength slit in nonsymmetric metallic gratings," *Opt. Lett.*, vol. 35, 2010, Art. no. 2597.
[17] A. E. Serebryannikov, "One-way diffraction effects in photonic crystal gratings made of isotropic materials," *Phys. Rev. B*, vol. 80, 2009, Art. no. 155117.
[18] C. C. Lu, X. Y. Hu, H. Yang, and Q. H. Gong, "Ultrahigh-contrast and wideband nanoscale photonic crystal all-optical diode," *Opt. Lett.*, vol. 36, no. 23, pp. 4668–4670, 2011.
[19] C. Wang, C. Z. Zhou, and Z. Y. Li, "On-chip optical diode based on silicon photonic crystal heterojunctions," *Opt. Exp.*, vol. 19, no. 27, pp. 26948–26955, 2011.
[20] Y. Zhang, Q. Kan, and G. P. Wang, "One-way optical transmission in silicon grating-photonic crystal structures," *Opt. Lett.*, vol. 39, 2014, Art. no. 4934.
[21] B. Maune *et al.*, "Liquid-crystal electric tuning of a photonic crystal laser," *Appl. Phys. Lett.*, vol. 85, pp. 360–362, 2004.
[22] M. A. Elrabiaey, N. F. F. Areed, and S. S. A. Obayya, "Novel plasmonic data storage based on nematic liquid crystal layers," *Lightw. Technol., J.*, vol. 34, no. 16, pp. 3726–3732, Aug. 2016.
[23] N. F. F. Areed and S. S. A. Obayya, "Novel all-optical liquid photonic crystal router," *IEEE Photon. Technol. Lett.*, vol. 25, no. 13, pp. 1254–1257, Oct. 2013.
[24] D.-K. Yang and S.-T. Wu, *Fundamentals of Liquid Crystal Devices*. Hoboken, NJ, USA: Wiley, 2006.
[25] M. F. O. Hameed, S. S. A. Obayya, K. Al-Begain, M. I. Abo el Maaty, and A. M. Nasr, "Modal properties of an index guiding nematic liquid crystal based photonic crystal fiber," *IEEE J. Lightw. Technol.*, vol. 27, no. 21, pp. 4754–4762, Nov. 2009.
[26] M. F. O. Hameed, S. S. A. Obayya, and H. A. El-Mikati, "Highly nonlinear birefringent soft glass photonic crystal fiber with liquid crystal core," *IEEE Photon. Technol. Lett.*, vol. 23, no. 20, pp. 1478–1480, Oct. 2011.
[27] K. Busch, S. Lölkes, R. B. Wehrspohn, and H. Föll, *Photonic Crystals*. Weinheim, Germany: Wiley-VCH, 2004.
[28] (2016). [Online]. Available: www.lumerical.com/tcad-products/fdtd/
[29] N. F. F. Areed and S. S. A. Obayya, "Novel design of symmetric photonic bandgap based image encryption system," *J. Prog. Electromagn. Res. C30*, pp. 225–239, 2012.
[30] R. S. Khandpur, *Handbook of Biomedical Instrumentation*. New York, NY, USA: McGraw-Hill, 2015.
[31] M. F.O. Hameed, A. M. Heikal, and S. S. A. Obayya, "Novel passive polarization rotator based on spiral photonic crystal fiber," *IEEE Photon. Technol. Lett.*, vol. 25, no. 16, pp. 1578–1581, Aug. 15, 2013.
[32] A. M. Abdelghani, N. F. F. Areed, M. F. O. Hameed, M. A. el Hamid Hindy, and S. S. A. Obayya, "Design of UWB antenna using reconfigurable optical router," *J. Opt. Quantum Electron.*, vol. 47, no. 8, pp. 2675–2688, 2015.
[33] N. F. F. Areed, S. S. A. Obayya, and H. A. El-Mikati, "Implementation of photonic crystal couplers," in *Proc. Nat. Radio Sci. Conf.*, pp. 1–8, 2007.
[34] M. Saleh, M. F.O. Hameed, N. F. F. Areed, and S. S. A Obayya, "Analysis of highly sensitive photonic crystal biosensor for glucose monitoring," *Appl. Comput. Electromagn. Soc. J.*, vol. 31, no. 7, pp. 836–842, 2016.
[35] R. M. Younis, N. F. F. Areed, and S. S. A Obayya, "Fully integrated AND and OR optical logic gates," *IEEE Photon. Tech. Lett.*, vol. 26, no. 19, pp. 1900–1903, Oct. 2014.
[36] S. S. A. Obayya, N. F. F. Areed, M. F. O. Hameed, and M. Hussein, "Optical nano-antennas for energy harvesting," in *Innovative Materials and Systems for Energy Harvesting Applications*, Hershey, PA, USA: IGI Global, 2015.
[37] S. S. A. Obayya, M. F. O. Hameed, and N. F. F. Areed, *Computational Liquid Crystal Photonics: Fundamentals, Modelling and Applications*. Hoboken, NJ, USA: Wiley, 2016.
[38] A. Bedoya *et al.*, "Reconfigurable photonic crystal waveguides created by selective liquid infiltration," *Opt. Exp. J.*, vol. 20, no. 10, pp. 11046–11056, 2012.
[39] (2016). [Online]. Available: https://www.comsol.com/
[40] Y. Jeong, B. Yang, B. Lee, H. S. Seo, S. Choi, and K. Oh, "Electrically controllable long-period liquid crystal fiber gratings," *IEEE Photon. Technol. Lett.*, vol. 12, no. 5, pp. 519–521, May 2000.